

Conformal Magnetic Composite RFID for Wearable RF and Bio-Monitoring Applications

Li Yang, *Student Member, IEEE*, Lara J. Martin, *Member, IEEE*, Daniela Staiculescu, *Member, IEEE*, C. P. Wong, *Fellow, IEEE*, and Manos M. Tentzeris, *Senior Member, IEEE*

Abstract—This paper introduces for the first time a novel flexible magnetic composite material for RF identification (RFID) and wearable RF antennas. First, one conformal RFID tag working at 480 MHz is designed and fabricated as a benchmarking prototype and the miniaturization concept is verified. Then, the impact of the material is thoroughly investigated using a hybrid method involving electromagnetic and statistical tools. Two separate statistical experiments are performed, one for the analysis of the impact of the relative permittivity and permeability of the proposed material and the other for the evaluation of the impact of the dielectric and magnetic loss on the antenna performance. Finally, the effect of the bending of the antenna is investigated, both on the S -parameters and on the radiation pattern. The successful implementation of the flexible magnetic composite material enables the significant miniaturization of RF passives and antennas in UHF frequency bands, especially when conformal modules that can be easily fine-tuned are required in critical biomedical and pharmaceutical applications.

Index Terms—Conformal antennas, magnetic composites, miniaturization, RF identification (RFID), RF passives, statistical tools, UHF, wearable applications.

I. INTRODUCTION

THE DEMAND for flexible miniaturized RF identification (RFID) tags has rapidly increased due to the requirements of automatic identification in various areas, such as item-level tracking and patient life-signs monitoring [1], [2]. The technology for RFID systems continuously improves and extends to structures of nonplanar shapes and to conformal sensors for wireless body-area networks (WBANs) [3]. Also, there is an increased demand for miniaturization, potentially addressed by the choice of substrate material, particularly magnetic materials [4]. The magnetic materials allow the miniaturization of the circuits without the use of a very large dielectric constant substrate. 3-D transponder antennas that utilize wound coil inductors do

make use of magnetic cores, but they are quite bulky and impractical. On the other side, flexible magnetic materials for two-dimensional embedded conformal planar antennas have not yet been successfully realized for standard use. This paper introduces for the first time a novel, mechanically flexible magnetic composite for printed circuits and two-dimensional antennas, which can reap the same miniaturization and tuning benefits as the nonflexible magnetic cores used for three-dimensional antennas.

One of the most significant challenges for applying new magnetic materials is understanding the interrelationships of the properties of the new materials with the design and performance of the specific topology (e.g., radiation pattern, scattering parameters). In previous studies, it has often been cited that the objectives of miniaturization and improved performance are tempered by the limited availability of materials that possess the required magnetic properties, while maintaining an acceptable mechanical and conformality performance [5]. Recently, formulation of nano-size ferrite particles has been reported [6] and formulation of magnetic composites comprised of ferrite filler and organic matrix has been demonstrated [7]. The implication of new magnetic materials has yet not been investigated for specific electromagnetic (EM) systems above the low megahertz range. Additionally, in the cases of complex microwave systems involving numerous interconnects, dielectric interfaces or radiating structures, the simultaneous optimization of the structure geometry along with the material may be necessary in order to achieve the optimal targeted performance. The aim of this work is to provide a basis for this co-design of materials and electromagnetic structures, namely for the benchmarking case of a novel flexible magnetic composite, a BaCo ferrite-silicone composite, and a UHF RFID antenna, respectively. Compared with the lower frequency tags operating in the LF and HF bands that suffer from limited read range, RFID tags operating in the UHF band are forecast to find the widest use due to their higher read range and higher data transfer rate in a more miniaturized size [8]. The UHF RFID bands vary in frequency, power levels, number of channel and sideband spurious limits of the RFID readers signal, depending on the application and the area of operation, such as 866–956 MHz in North America/Europe for EPC GEN2 item-level tracking and the lower band around 400 MHz for bio-applications.

Specifically, in this study, a benchmark structure was first designed for 480 MHz in a full-wave simulator for an unfilled silicone substrate; then the magnetic particles, namely the Co_2Z powder from Trans-Tech, were added and the same antenna was redesigned for 480 MHz by reducing its physical size, thus

Manuscript received April 25, 2008; revised July 24, 2008. First published November 18, 2008; current version published December 05, 2008. This work was supported by the Georgia Electronic Design Center and by the National Science Foundation under NSF CAREER Grant ECS-0801798 and NSF Grant ECS-0313951.

L. Yang, D. Staiculescu, and M. M. Tentzeris are with the School of Electrical and Computer Engineering, Georgia Institute of Technology, Atlanta, GA 30332 USA (e-mail: LiYang@ece.gatech.edu).

L. J. Martin is with Motorola Inc., Plantation, FL 33322 USA.

C. P. Wong is with the Packaging Research Center and School of Materials Science and Engineering, Georgia Institute of Technology, Atlanta, GA 30332 USA.

Color versions of one or more of the figures in this paper are available online at <http://ieeexplore.ieee.org>.

Digital Object Identifier 10.1109/TMTT.2008.2006810

proving the miniaturization concept. It is well known that the size of the antenna is inversely proportional to the square root of the product of effective permittivity and effective permeability. Therefore, a nonmagnetic material would have to have a permittivity close to about 18 to give comparable miniaturization capability, which is high compared to the permittivity of 7.14 for the magnetic material used in this work. The next step was the fabrication of the material and the measurement of the dielectric and magnetic characteristics, including loss. The benchmarking miniaturized antenna was fabricated on the magnetic composite and its performance was measured validating the simulations with the measured data [9]. Furthermore, the impact of the material on the system-level performance of the antenna was thoroughly investigated using a hybrid method including electromagnetic simulators and statistical tools: first, the very important issue of dielectric and magnetic losses, then both the relative permittivity and permeability. Finally, the performance of the antenna when conformed on a foam cylinder was measured, both the S -parameters and radiation pattern, and it was concluded that the antenna is still functional even for a tight bending radius of 27 mm. Magnetic materials can provide RF designers with increased options in their system design, especially if their effects are better understood. This detailed analysis of the system-level impact of the electrical parameters of the magnetic composite attempts to bring more understanding and to enable a more extensive future use of such materials. The presented magnetic substrate is the first flexible magnetic composite tested and proven for the 480 MHz bandwidth (BW) with acceptable magnetic losses, which makes it usable for lightweight conformal/wearable applications like pharmaceutical industry and wireless health monitoring in hospital, ambulance and home-based patient care, as well as wearable communication and authentication devices.

II. MATERIAL DEVELOPMENT

The first step for this work was to develop a magnetic composite that provides the advantage of low-temperature processing for compatibility with organic substrate processing, mechanical flexibility, and high adhesion. With regard to these three properties, the magnetic composite would have to be compatible with common substrates used for RFID, such as polyethylene terephthalate (PET) and polyimide. Additionally, the composite dielectric loss can affect circuit performance, thus low dielectric loss should be targeted. For these objectives, the properties of candidate materials should include low-temperature processability, high mechanical flexibility, high adhesion, and low dielectric loss. Dielectric constant can also affect the circuit performance and should be carefully monitored. The matrix materials considered candidates for this proposed work included silicone and benzocyclobutene (BCB). Silicone provides reasonable viscosities required for good filler mixing during processing, that is, not too low to promote settling and not too high for uniform mixing. Additionally, silicone provides the properties of mechanical flexibility and, for some formulations, good adhesion.

After careful analysis, the matrix material was chosen to be Dow Corning Sylgard 184 silicone. The dielectric parameters of the unfilled silicone, used in the initial antenna design, are $\epsilon_r =$

TABLE I
MEAN AND 95% CONFIDENCE INTERVALS FOR ϵ AND μ
MEASUREMENTS OF FERRITE COMPOSITE AT 480 MHz

	<i>mean</i>	<i>Lower CI</i>	<i>Upper CI</i>
ϵ_r	7.142	7.083	7.201
μ_r	2.463	2.457	2.468
$\tan\delta_\epsilon$	0.0017	0.0005	0.0028
$\tan\delta_\mu$	0.0391	0.0358	0.0424

2.65 and $\tan\delta_\epsilon = 0.001$. The choice for the magnetic composite was Co_2Z powder supplied by Trans-Tech. A 40 vol% ferrite paste was produced with a mixer at 240 rpm (rotations per minute) and 110 °C for 30 minutes. The paste was transferred into a flat mold and vacuum cured with a hold confirmed to occur at > 125 °C for 50 min to produce a 1.3 mm thick substrate.

The material was measured using an HP4291A impedance analyzer to obtain complex permittivity (ϵ) and permeability (μ) (real and imaginary parts) with material fixtures 16453A for ϵ and 16454A for μ over the frequency range of 1 MHz to 1.8 GHz. There were 5 measurements taken for each ϵ_r , μ_r , $\tan\delta_\epsilon$ and $\tan\delta_\mu$. The summary statistics, including the mean and 95% C.I. (confidence intervals) for ϵ_r , μ_r , $\tan\delta_\epsilon$ and $\tan\delta_\mu$ of the ferrite composite at 480 MHz are given in Table I. Based on these results, the values used in the model were $\epsilon_r = 7.14$, $\mu_r = 2.46$, $\tan\delta_\epsilon = 0.0017$, and $\tan\delta_\mu = 0.039$.

III. ANTENNA DESIGN AND MEASUREMENT

One of the main challenges in designing an RFID tag is the impedance matching between the terminals of the tag antenna and those of the IC. This requires a conjugate matching technique, such as series or parallel stubs and/or using inductively coupling. The matching network of the tag has to guarantee the maximum power delivered to the IC, which is used to store the data transmitted to and receive from the RFID reader. The return loss (RL) of RFID antenna can be calculated based on the power reflection coefficient which takes into account the reactance part of the IC impedance [10]

$$|S|^2 = \left| \frac{Z_{IC} - Z_{ANT}^*}{Z_{IC} + Z_{ANT}} \right|^2 \quad (1)$$

where Z_{IC} represents the impedance of the IC and Z_{ANT} represents the impedance of the antenna terminals with Z_{ANT}^* being its complex conjugate.

Another challenge is the dimensions of the RFID tag. The free space wavelength at 480 MHz is 625 mm. For an application as wristband patient monitoring, it is clear that the miniaturization of the tag becomes a priority.

To verify the miniaturization benefits of the presented magnetic composite, a folded bow-tie meander line dipole antenna was designed and fabricated on the characterized magnetic composite material substrate. The RFID prototype structure is shown in Fig. 1 along with dimensions, with the IC placed in the center of the shorting stub arm.

The nature of the bow-tie shape of the half-wavelength dipole antenna body allows for a more broadband operation [11]. The meander line helps further miniaturizing the antenna structure [12]. The shorting stub arm is responsible for the matching of

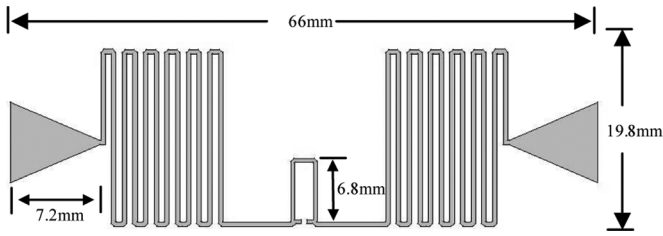


Fig. 1. Configuration of the RFID tag module on magnetic composite substrate.

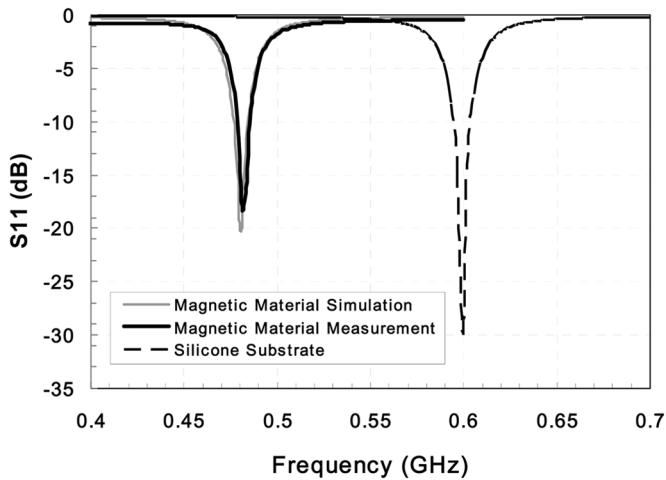


Fig. 2. Measured and simulated RL of the RFID tag antenna on the magnetic material with the comparison of the one on the silicone substrate.

the impedance of the antenna terminals to that of the IC through the fine tuning of the length.

Next, a GS 1000 μm pitch probe was used for impedance measurements. In order to minimize backside reflections, the fabricated antenna was placed on a custom-made probe station using high density polystyrene foam with low relative permittivity of value 1.06, resembling that of the free space. The calibration method used was short-open-load-thru (SOLT). The initial structure was designed for the lower end of the UHF spectrum and was modeled using Zeland IE3D full wave EM software. The initial substrate was pure silicone ($\epsilon_r = 2.65$ and $\tan \delta_\epsilon = 0.001$) of 1.3 mm thickness. The same dimensions of the antenna were maintained for the magnetic composite material. The RL plot is shown in Fig. 2, demonstrating a frequency down shifting of 20% due to the enhanced combined relative permeability and relative permittivity, which proves the miniaturization concept. Fig. 2 shows a very good agreement for the simulations versus measurements for the antenna on the magnetic composite.

The radiation pattern comparison of simulation versus measurements of the RFID tag module on magnetic substrate is shown in Fig. 3, showing good agreement. The radiation pattern is almost uniform (omnidirectional) at 480 MHz with a gain around -4.63 dBi.

IV. MAGNETIC COMPOSITE IMPACT ON ANTENNA PERFORMANCE

One of the most critical factors in the magnetic composite fabrication was the control of the permittivity and permeability

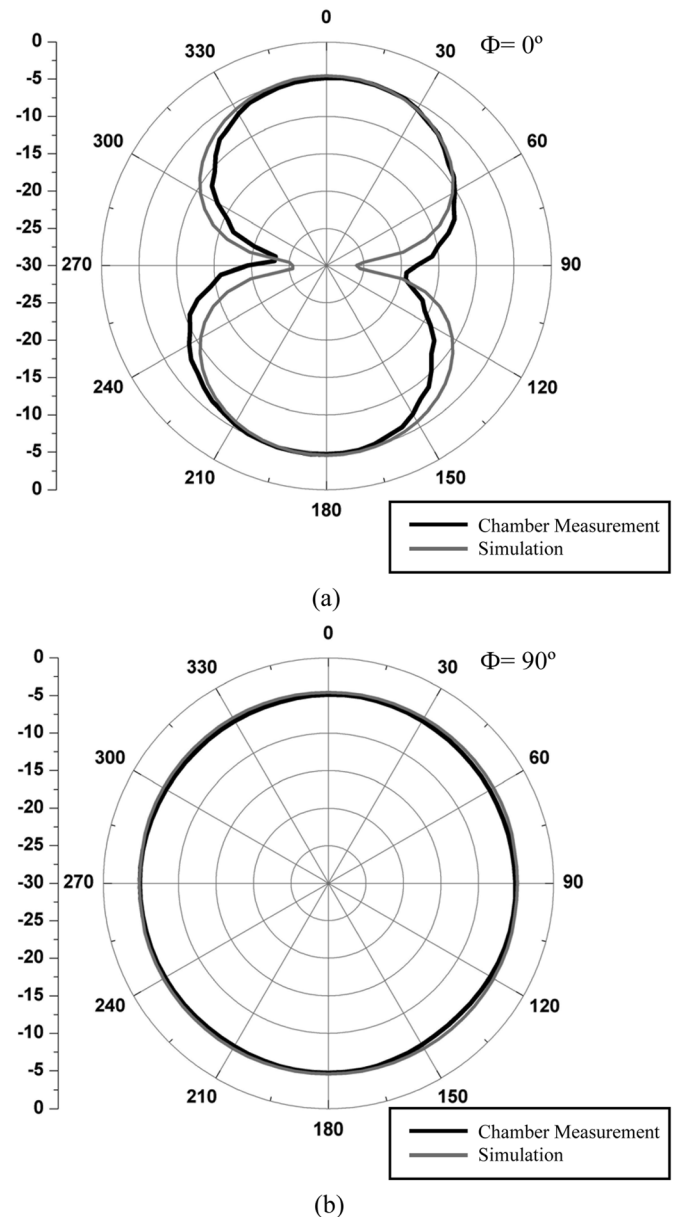


Fig. 3. Simulated versus measured 2-D radiation plots for: (a) $\phi = 0^\circ$ and (b) $\phi = 90^\circ$.

values, so a careful analysis of the impact of both the dielectric and magnetic performance based on the fabrication variability was necessary. These material properties are not mutually exclusive. The permittivity [13] and permeability [14] are both governed by the molecular arrangement (lattice structure) and elemental composition of the material, which prevents the tuning of these properties independently. So the following analysis does not attempt to optimize the material parameters, but rather to quantify the effect of the parameters on the system-level performance of the antenna.

First, the impact of the loss tangents was investigated. The methodology used involves electromagnetic simulations and statistical tools and is presented as a flowchart in Fig. 4. First, a design of experiments (DOE) [15] is performed to develop the first order (linear) statistical model, including both loss tangents, dielectric and magnetic. Then, the model is checked

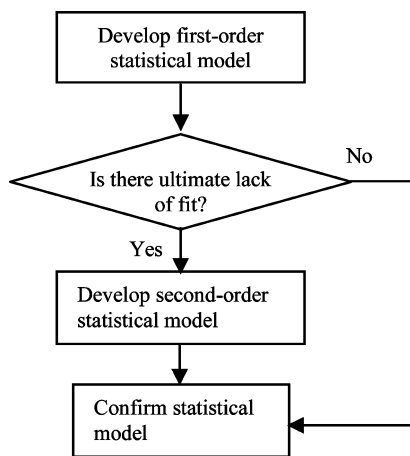


Fig. 4. Procedure for statistical model development.

for ultimate lack of fit, more specifically, if curvature might be present in the output response. If curvature in the response is detected, the analysis is extended to additional points indicated by the response surface methodology (RSM) [15] which can account for curvature through second-order model development. Usually, these second-order models are reasonable approximations of the true functional relationship over relatively small regions. Once validated using statistical diagnostic tools, the models approximate the actual system within the defined design space. Hybrid methods including statistical tools and EM simulations have been extensively used for RF and microwave systems analysis and optimization [16].

The statistical experimentation method chosen for the first-order statistical model is a full factorial DOE with center points [15]. The factorial designs are used in statistical experiments involving several (k) factors where the goal is the study of the joint effects of the factors on a response and the elimination of the least important ones from further optimization iterations. The 2^k factorial design is the simplest one, with k factors at two levels each. It provides the smallest number of runs for studying k factors and is widely used in factor screening experiments [15]. Center points are defined at the center of the design space and enable investigating validity of the model, including curvature in the response, and account for variations in the fabrication process of the structure. Since the statistical models are based on deterministic simulations, the variations of the center points were statistically simulated assuming a 3σ process with a $\pm 2\%$ tolerance for both $\tan \delta_\epsilon$ and $\tan \delta_\mu$.

In this case, since we have two input variables, a 2^2 full factorial DOE was performed for the first-order statistical model, with the following four output variables as the antenna performance figures of merit: resonant frequency f_{res} , minimum RL, maximum gain at 480 MHz G , and the 10 dB BW. The ranges of the input variables are presented in Table II, while ϵ_r and μ_r have been kept at their nominal values of 7.14 and 2.46 respectively.

The first-order models showed curvature in all of the responses, and RSM was needed for the second-order statistical model. Validation of the models was investigated, with all but the BW validated for the normality assumption, and the equal variance was validated for RL and G , but not for f_{res} and BW.

TABLE II
RANGES FOR THE INPUT VARIABLES

Variable	Low value “-“	High value “+”	Center point
$\tan \delta_\epsilon$	0.00136	0.00204	0.0017
$\tan \delta_\mu$	0.0312	0.0468	0.039

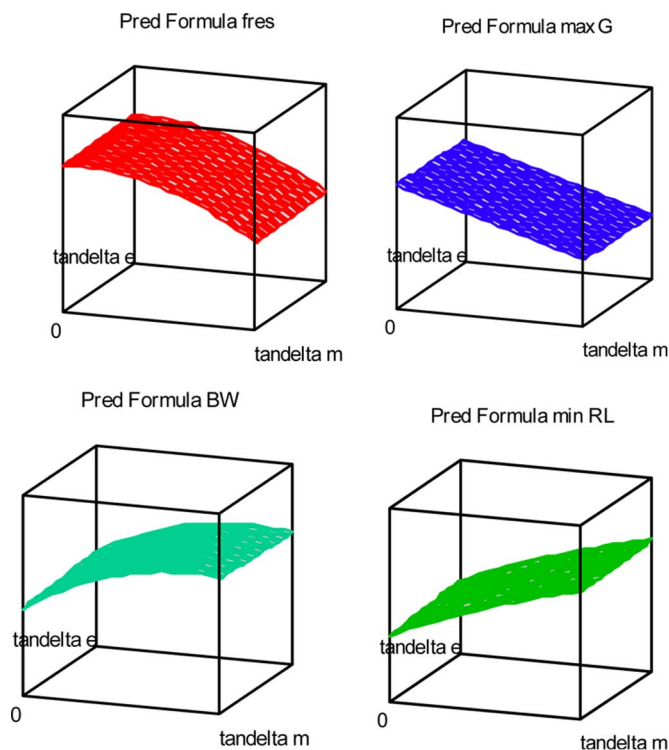


Fig. 5. Surfaces of possible solutions for outputs.

The four models are given by (2)–(5). An interesting result is the fact that the resonant frequency is not dependent upon $\tan \delta_\epsilon$. This is due to the fact that the interval of analysis of $\tan \delta_\epsilon$ shown in Table II, chosen based on the real material, is of an order of magnitude smaller than $\tan \delta_\mu$, because $\tan \delta_\epsilon$ is of an order of magnitude smaller than $\tan \delta_\mu$ and the intervals are chosen to be 20% up and down the center point value. However, when reflected in loss and BW in (3)–(5), even the much smaller $\tan \delta_\epsilon$ becomes significant.

The models allow for the “a priori” prediction of the antenna performance with respect to either figure of merit or all simultaneously allocating any weight factors to each one of them. The goals chosen in this case were a specific f_{res} of 480 MHz (center point value), maximum gain G , minimum RL, and maximum BW, all with equal weight. The surfaces for the four figures of merit as a function of the input parameters are presented in Fig. 5, indicating the curvature in the models. The values that satisfied the four goals within the ranges presented in Table II were $\tan \delta_\epsilon = 0.00136$ and $\tan \delta_\mu = 0.032427$, leading to the predicted values of the four figures of merit of $f_{\text{res}} = 480.48$ MHz, $\text{RL} = -22.97$ dB, $G = -4.32$ dBi and $\text{BW} = 7.63$ MHz. So, ideally, these values of the loss tangents would provide optimal performance of the antenna for the above mentioned goals. The models indicate that the resonant frequency decreases with the losses, as the gain and the RL obviously degrade. For the BW, although the model is significant

and shows an increase of the BW with dielectric loss, the absolute numbers in the RSM vary only between 7.61–7.7 MHz, which is not a large difference for practical applications.

The consideration of the relative permeability in the antenna design requires a more detailed analysis of its impact, together

TABLE III
RANGES FOR THE INPUT VARIABLES

Variable	Low value “-“	High value “+“	Center point
ϵ_r	5.712	8.568	7.14
μ_r	1.968	2.952	2.46

$$f_{\text{res}}(\text{MHz}) = 480.47 - 0.024 \left(\frac{\tan \delta_m - 0.039}{0.0078} \right) - 0.013 \left(\frac{\tan \delta_m - 0.039}{0.0078} \right)^2 \quad (2)$$

$$\text{RL}(\text{dB}) = -20.34 + 0.18 \left(\frac{\tan \delta_e - 0.0017}{0.00034} \right) + 2.48 \left(\frac{\tan \delta_m - 0.039}{0.0078} \right) - 0.062 \left(\frac{\tan \delta_m - 0.039}{0.0078} \right)^2 - 0.43 \left(\frac{\tan \delta_e - 0.0017}{0.00034} \right)$$

$$\times \left(\frac{\tan \delta_m - 0.039}{0.0078} \right) \quad (3)$$

$$G(\text{dBi}) = -4.57 - 0.019 \left(\frac{\tan \delta_e - 0.0017}{0.00034} \right) - 0.26 \left(\frac{\tan \delta_m - 0.039}{0.0078} \right) - 0.0044 \left(\frac{\tan \delta_m - 0.039}{0.0078} \right)^2 + 0.0005 \left(\frac{\tan \delta_e - 0.0017}{0.00034} \right) \times \left(\frac{\tan \delta_m - 0.039}{0.0078} \right) \quad (4)$$

$$\text{BW}(\text{MHz}) = 7.69 + 0.0000088 \left(\frac{\tan \delta_e - 0.0017}{0.00034} \right) + 0.038 \left(\frac{\tan \delta_m - 0.039}{0.0078} \right) - 0.031 \left(\frac{\tan \delta_m - 0.039}{0.0078} \right)^2 - 0.005 \left(\frac{\tan \delta_e - 0.0017}{0.00034} \right) \times \left(\frac{\tan \delta_m - 0.039}{0.0078} \right) \quad (5)$$

with the relative permittivity, on the antenna performance. The next statistical experiment analyzes the impact of these two parameters on the same major antenna outputs: resonant frequency f_{res} , minimum RL, maximum gain at the resonant frequency G , and the 10 dB BW.

The methodology used is the same as the one used for the loss tangent analysis and shown in Fig. 4.

In this case, since we have two input variables, the same 2^2 full factorial DOE was performed for the first-order statistical model, with the ranges of the input variables presented in Table III, while $\tan \delta_e$ and $\tan \delta_m$ have been kept at their nominal values of 0.0017 and 0.039, respectively.

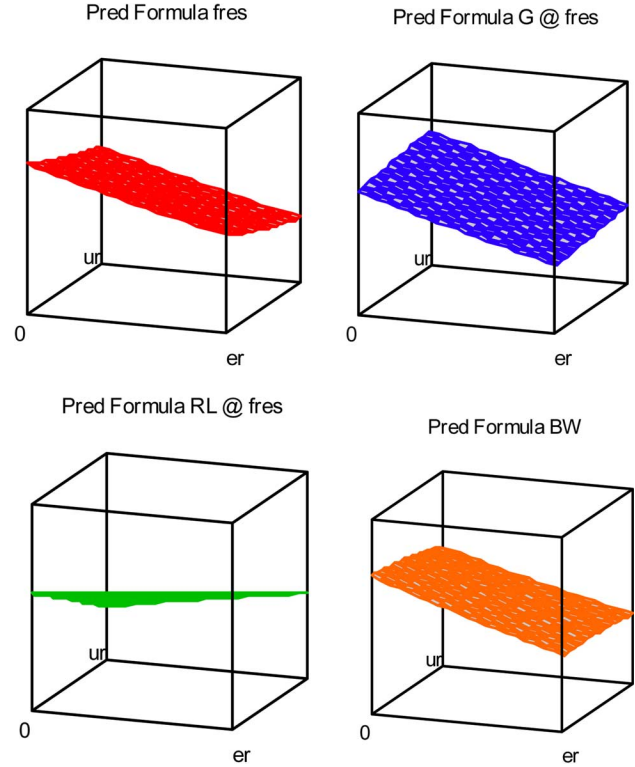


Fig. 6. Surfaces of possible solutions for outputs.

The first order models showed curvature in all of the responses, and RSM was needed for the second-order statistical model. The validation of the models was investigated. For the normality of residuals assumption, all models but G have normally distributed residuals. For the validation of the equal variance of residuals assumption, all the models had equal variance of residuals. The four models are given by (6)–(9).

The antenna performance was predicted again for the same goals: f_{res} of 480 MHz (center point value), maximum gain G , minimum RL, and maximum BW, all with equal weight. The surfaces for the four figures of merit as a function of the input parameters are presented in Fig. 6, indicating slight curvature in the models. The values that satisfied the four conditions within the ranges presented in Table III were $\epsilon_r = 6.41$ and $\mu_r = 2.95$, leading to the values of the four figures of merit of $f_{\text{res}} = 480.56$ MHz, $\text{RL} = -24.08$ dB, $G = -4.42$ dBi and $\text{BW} = 7.73$ MHz. The models indicate that the resonant frequency decreases with the relative permittivity and permeability, which again proves the miniaturization concept. For the BW and the gain, although the models are significant, the absolute numbers in the RSM vary only between 7.23–8.22 MHz for the BW and 4.27–4.81 dBi for the gain, which are not large differences for practical applications.

As reported above, the analysis does not attempt to optimize

$$f_{\text{res}}(\text{MHz}) = 480.61 - 15.19 \left(\frac{\epsilon_r - 7.14}{1.428} \right) - 9.5 \left(\frac{\mu_r - 2.64}{0.492} \right) + 1.01 \left(\frac{\epsilon_r - 7.14}{1.428} \right)^2 + 1.46 \left(\frac{\mu_r - 2.64}{0.492} \right)^2 \quad (6)$$

$$\text{RL}(\text{dB}) = -20.34 + 1.19 \left(\frac{\epsilon_r - 7.14}{1.428} \right) - 2.78 \left(\frac{\mu_r - 2.64}{0.492} \right) + 0.39 \left(\frac{\epsilon_r - 7.14}{1.428} \right) \left(\frac{\mu_r - 2.64}{0.492} \right) - 0.14 \left(\frac{\epsilon_r - 7.14}{1.428} \right)^2 - 0.11 \left(\frac{\mu_r - 2.64}{0.492} \right)^2 \quad (7)$$

$$G(\text{dBi}) = -4.56 - 0.19 \left(\frac{\epsilon_r - 7.14}{1.428} \right) + 0.032 \left(\frac{\mu_r - 2.64}{0.492} \right) + 0.0087 \left(\frac{\epsilon_r - 7.14}{1.428} \right)^2 + 0.0024 \left(\frac{\mu_r - 2.64}{0.492} \right)^2 \quad (8)$$

$$\text{BW}(\text{MHz}) = 7.68 - 0.35 \left(\frac{\epsilon_r - 7.14}{1.428} \right) - 0.09 \left(\frac{\mu_r - 2.64}{0.492} \right) + 0.037 \left(\frac{\epsilon_r - 7.14}{1.428} \right) \left(\frac{\mu_r - 2.64}{0.492} \right) + 0.022 \left(\frac{\epsilon_r - 7.14}{1.428} \right)^2 - 0.029 \left(\frac{\mu_r - 2.64}{0.492} \right)^2 \quad (9)$$

the material parameters, but rather to quantify the effect of the parameters on the system-level performance of the antenna. Even if the two values of $\tan \delta_\epsilon = 0.00136$ and $\tan \delta_\mu = 0.032427$ or $\epsilon_r = 6.41$ and $\mu_r = 2.95$ cannot be achieved simultaneously, this analysis gives a thorough understanding of the effects and provides the designer with a systematic approach in choosing the materials and the antenna geometry.

V. CONFORMAL PERFORMANCE

In order to verify the performance of the proposed RFID antenna in conformal applications, measurements were performed by conforming the same RFID tag onto a foam cylinder, as shown in Fig. 7. The radius of the cylinder was chosen to be very small at 27 mm, in order to explore the limits of the design. The

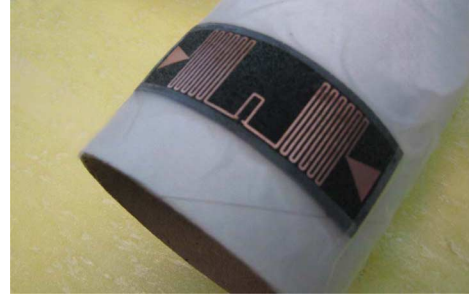


Fig. 7. Conformal RFID tag on a foam cylinder.

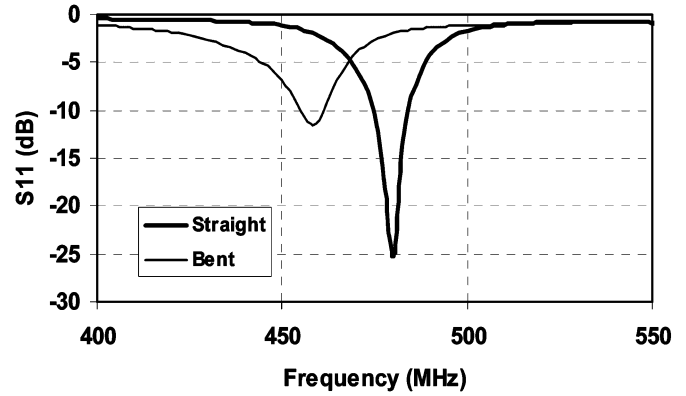


Fig. 8. Measured RL of the flat RFID tag and the conformal RFID tag. 20 MHz frequency down shifting is observed.

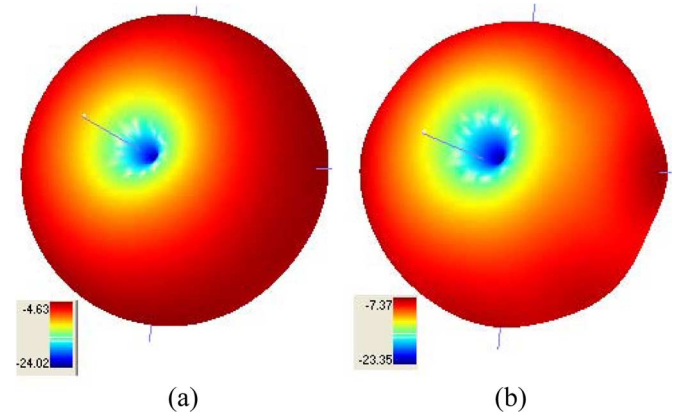


Fig. 9. Measured radiation pattern of: (a) the flat RFID tag and (b) the conformal RFID tag. Max gain drops from -4.63 to -7.37 dBi.

result in Fig. 8 shows that the RL of the fabricated antenna is shifted down by 22 MHz with a center frequency at 458 MHz. Previous results [9] showed a shift of 6 MHz for a lower curvature of 54 mm radius, which proves that the shift is increasing with the curvature level. Overall, the antenna still has good performance if the shift in frequency is considered at the beginning of the design process, even for such a large bend. Fig. 9 shows the radiation patterns for the straight and conformal antennas. The doughnut shape is slightly degraded for the conformal antenna and the maximum gain drops from -4.63 to -7.37 dBi.

The flexible nature of the proposed substrate enables the RFID tag module's application in various areas. Fig. 10 demonstrates the conformal RFID tag prototype in the applications



Fig. 10. Embodiments of the conformal RFID tag prototype in the applications of wireless health monitoring and pharmaceutical drug bottle tracking.

of wireless health monitoring and pharmaceutical drug bottle tracking.

VI. CONCLUSION

This work is the first demonstration of a flexible magnetic composite proven for the 480 MHz BW with acceptable magnetic losses that makes it usable for small size, lightweight conformal applications like wireless health monitoring in pharmaceuticals, hospital, ambulance and home-based patient care. A combination of electromagnetic tools and measurements has been used to investigate the impact of magnetic composite materials to the miniaturization of RFID antennas considering geometric and material parameters, as well as conforming radius. This approach has been applied to the design of a benchmarking conformal RFID tag module and has enabled the assessment of implication that the choice of materials have on this design, specifically the antenna miniaturization by using the magnetic composite versus pure silicone. A real composite material has been fabricated and the performance of the miniaturized antenna predicted using the models. Next, the important issues of the dielectric and magnetic losses has been addressed by performing a thorough statistical analysis to investigate the impact of the losses on the antenna performance. Furthermore, since the permeability was first introduced in this paper for a conformal antenna, the impact of the relative permeability in conjunction with relative permittivity were addressed together in another statistical analysis. The losses impact the resonant frequency, RL, and antenna gain, whereas the dielectric constant and magnetic property mostly decrease the resonant frequency, thus proving the miniaturization concept.

ACKNOWLEDGMENT

The authors wish to acknowledge the Georgia Electronic Design Center (GEDC). The authors extend special thanks to Dr. M. D. Hill and B. W. Treadway, both with Trans-Tech Inc., Adamstown, MD, D. J. Meyer, Motorola, Plantation, FL, for the help with the antenna fabrication, and K. Rutkowski, Satimo, Kennesaw, GA, for the radiation pattern measurements.

REFERENCES

- [1] K. Finkenzeller, *RFID Handbook*, 2nd ed. New York: Wiley, 2004.
- [2] A. Cangialosi, J. E. Monaly, and S. C. Yang, "Leveraging RFID in hospitals: Patient life cycle and mobility perspectives," *IEEE Commun. Mag.*, vol. 45, no. 9, pp. 18–23, Sep. 2007.
- [3] G. Marrocco, "RFID antennas for the UHF remote monitoring of human subjects," *IEEE Trans. Antennas Propag.*, vol. 55, no. 6, pp. 1862–1870, Jun. 2007.
- [4] "Magnetic materials for RFID," TechnoForum, TDK, Tokyo, Japan, 2005. [Online]. Available: http://www.tdk.com/jp/ft2005/pdf_e/2f0215e.pdf
- [5] N. Das and A. K. Ray, "Magneto optical technique for beam steering by ferrite based patch arrays," *IEEE Trans. Antennas Propag.*, vol. 49, no. 8, pp. 1239–1241, Aug. 2001.
- [6] S. Morrison, C. Cahill, E. Carpenter, S. Calvin, R. Swaminathan, M. McHenry, and V. Harris, "Magnetic and structural properties of nickel zinc ferrite nanoparticles synthesized at room temperature," *J. Appl. Phys.*, vol. 95, no. 11, pp. 6392–6395, Jun. 2004.
- [7] H. Dong, F. Liu, Q. Song, Z. J. Zhang, and C. P. Wong, "Magnetic nanocomposite for high Q embedded inductor," in *IEEE Int. Adv. Packag. Mate., Process, Properties, Interfaces Symp. and Exhibition*, Atlanta, GA, Mar. 2004, pp. 171–174.
- [8] A. Rida, L. Yang, R. Vyas, S. Bhattacharya, and M. M. Tentzeris, "Design and integration of inkjet-printed paper-based UHF components for RFID and ubiquitous sensing applications," in *Eur. Microw. Conf.*, Oct. 9–12, 2007, pp. 724–727.
- [9] L. Yang, L. Martin, D. Staiculescu, C. P. Wong, and M. M. Tentzeris, "A novel flexible magnetic composite RFID for wearable RF and bio-monitoring applications," in *IEEE MTT-S Int. Microw. Symp. Dig.*, Atlanta, GA, Jun. 2008, pp. 963–966.
- [10] P. V. Nikitin, S. Rao, S. F. Lam, V. Pillai, and H. Heinrich, "Power reflection coefficient analysis for complex impedances in RFID tag design," *IEEE Trans. Microw. Theory Tech.*, vol. 53, no. 9, pp. 2721–2725, Sep. 2005.
- [11] A. Hung, S. Wong, and W. Ismail, "RFID transponder using bow tie antenna for wireless application," in *Int. RF Microw. Conf.*, Sep. 12–14, 2006, pp. 21–25.
- [12] A. Galehdar, D. V. Thiel, S. G. O'Keefe, and S. P. Kingsley, "Efficiency variations in electrically small, meander line RFID antennas," in *IEEEAP-S Int. Symp.*, Jun. 9–15, 2007, pp. 2273–2276.
- [13] S. O. Kasap, *Principles of Electronic Materials and Devices*, 2nd ed. New York: McGraw-Hill, 2002, pp. 516–516.
- [14] L. L. Hench and J. K. West, *Principles of Electronic Ceramics*. New York: Wiley, 1990, pp. 296–296.
- [15] J. Neter *et al.*, *Applied Linear Statistical Models*, 4th ed. Chicago, IL: McGraw-Hill, 1996.
- [16] D. Staiculescu, C. You, L. Martin, W. Hwang, and M. M. Tentzeris, "Hybrid electrical/mechanical optimization technique using time-domain modeling, finite element method and statistical tools for composite smart structures," in *Proc. IEEE MTT-S Int. Microw. Symp. Dig.*, Jun. 2006, pp. 288–291.



Li Yang (S'04) received the B.S. and M.S. degrees in electronic engineering from Tsinghua University, Beijing, China, in 2002 and 2005, respectively, and is currently working toward the Ph.D. degree in electrical and computer engineering at the Georgia Institute of Technology, Atlanta.

He is a Graduate Research Assistant with the ATHENA Research Group, Georgia Electronic Design Center. His research interests include RFID technology, radio frequency integrated circuit (RFIC) technology, and the design of wireless transceivers

for sensing and power scavenging applications.

Mr. Yang was the recipient/corecipient of the 2008 IEEE Microwave Theory and Techniques Society (IEEE MTT-S) International Microwave Symposium (IMS) Student Paper Honorary Mention Award, the 2008 IEEE Antennas and Propagation (AP-S) Symposium Student Paper Honorary Mention Award, the 2007 IEEE AP-S Symposium Best Student Paper Award, the 2007 IEEE MTT-S IMS Third Best Student Paper Award, the 2007 ISAP Poster Presentation Award, and the 2006 Asia-Pacific Microwave Conference Award.



Lara J. Martin (M'98) received the Bachelor of Chemical Engineering, M.S. degree in materials science and engineering, and Ph.D. degree in materials science and engineering (with a minor in applied statistics) from the Georgia Institute of Technology, Atlanta.

She has used her background in both engineering and statistics throughout her career with Motorola Inc., Plantation, FL. She currently works as a Master Black Belt for Motorola Inc.'s Government and Public Safety business. She has authored or coauthored papers in several forums, including conference proceedings, peer-reviewed journals, and a cover story paper for a trade magazine. She holds U.S. and international patents.

Dr. Martin achieved a Six Sigma Black Belt in 2001 and became the 17th Master Black Belt recognized by Motorola Inc. in 2003 for her application of statistical tools and methods. In 2003, she was inducted as a Motorola Science Advisory Board associate member, representing the top 1.5% of the corporation's technical resources. Additionally, she was elected to the Georgia Institute of Technology Council of Outstanding Young Engineering Alumni in 2004 and was the recipient of the IEEE Components, Packaging, and Manufacturing Technology Outstanding Young Engineer of the Year Award in 2005.



Daniela Staiculescu (M'03) received the B.S. degree in electrical engineering from the Polytechnic University, Bucharest, Romania, in 1993, and the M.S. and Ph.D. degrees from the Georgia Institute of Technology, Atlanta, in 1999 and 2001, respectively.

From 2001 to 2003, she was with RF Solutions, Atlanta, GA. She is currently a Research Engineer with the ATHENA Group, Georgia Institute of Technology. She uses statistical techniques like design of experiments and response surface modeling for design rule development/optimization and for analysis of passive systems. She has authored or coauthored over 50 papers and coauthored a book chapter. She filed one invention disclosure. Her main research interest is wireless sensor networks for various applications, mostly for medical patient monitoring like ECG and coughless blood pressure. She is also interested in new materials, like liquid-crystal polymer (LCP), paper electronics, magnetic composites, and nanotechnology.



C. P. Wong (SM'87-F'92) received the B.S. degree from Purdue University, West Lafayette, IN, and the Ph.D. degree from the Pennsylvania State University, University Park.

He held a postdoctoral fellowship with Nobel Laureate Professor Henry Taube at Stanford University. He is currently a Regents' Professor and Holder of the Charles Smithgall Institute Endowed Chair (one of the two Institute Endowed Chairs at the Georgia Institute of Technology) with the School of Materials Science and Engineering, Georgia Institute of Technology, Atlanta. He was with AT&T for many years and was elected an AT&T Bell Laboratories Fellow in 1992. Since 1996, he has been a Professor with the School of Materials Science and Engineering, Georgia Institute of Technology. He was named a Regents' Professor in 2000, and named Holder of the Georgia Institute of Technology Institute endowed chair in 2005. He has authored or coauthored over 600 technical papers. He holds over 50 U.S. patents and numerous international patents.

Dr. Wong was the president of the IEEE Components, Packaging, and Manufacturing Technology (CPMT) Society (1992 and 1993). He is a member of the National Academy of Engineering since 2000. He has been the recipient of numerous awards, among those the AT&T Bell Laboratories Fellow Award in 1992, the IEEE CPMT Society Outstanding Sustained Technical Contributions Award in 1995, the Georgia Institute of Technology Sigma Xi Faculty Best Re-

search Paper Award in 1999, the Best M.S., Ph.D., and Undergraduate Thesis Awards in 2002 and 2004, respectively, the University Press (London) Award of Excellence, the IEEE Third Millennium Medal in 2000, the IEEE EAB Education Award in 2001, the IEEE CPMT Society Exceptional Technical Contributions Award in 2002, the Georgia Institute of Technology Outstanding Ph.D. Thesis Advisor Award, the IEEE Components, Packaging and Manufacturing Technology Field Award in 2006, the Sigma Xi's Monie Ferst Award in 2007, and the Society of Manufacturing Engineers (SME) TEEM Award in 2008. He was elected the Class of 1935 Distinguished Professor in 2004.



Manos M. Tentzeris (M'98-SM'03) received the Diploma degree in electrical and computer engineering from the National Technical University of Athens, Athens, Greece, in 1992, and the M.S. and Ph.D. degrees in electrical engineering and computer science from The University of Michigan at Ann Arbor, in 1993 and 1998, respectively.

He is currently an Associate Professor with the School of Electrical and Computer Engineering, Georgia Institute of Technology, Atlanta. He has authored or coauthored over 310 papers in refereed journals and conference proceedings, two books, and 15 book chapters. He has helped develop academic programs in highly integrated/multilayer packaging for RF and wireless applications, microwave microelectromechanical systems (MEMS), SOP integrated antennas and adaptive numerical electromagnetics (finite difference time domain (FDTD), multiresolution algorithms), and heads the ATHENA Research Group (20 researchers). He is the Georgia Institute of Technology National Science Foundation (NSF) Packaging Research Center Associate Director for RF Research and the RF Alliance Leader. He is also the leader of the Novel Integration Techniques Subthrust of the Broadband Hardware Access Thrust of the Georgia Electronic Design Center (GEDC) of the State of Georgia. During the summer of 2002, he was a Visiting Professor with the Technical University of Munich, Munich, Germany, where he introduced a course in the area of high-frequency packaging. He has given over 50 invited talks in the same area to various universities and companies in Europe, Asia, and the U.S.

Dr. Tentzeris is a member of URSI Commission D, an associate member of the European Microwave Association (EuMA), and a member of the Technical Chamber of Greece. He was the 1999 Technical Program co-chair of the 54th ARFTG Conference, Atlanta, GA, and he is the vice-chair of the RF Technical Committee (TC16) of the IEEE Components, Packaging, and Manufacturing Technology (CPMT) Society. He has organized various sessions and workshops on RF/Wireless Packaging and Integration in IEEE ECTC, International Microwave Symposium (IMS), and AP-S Symposia, for all of which he is a member of the Technical Program Committee (TPC) in the area of components and RF. He was the TPC Chair for the 2008 IEEE Microwave Theory and Techniques Society (IEEE MTT-S) IMS. He was the recipient of the 2003 National Aeronautics and Space Administration (NASA) Godfrey Art Anzic Collaborative Distinguished Publication Award for his activities in the area of finite-ground low-loss low-crosstalk CPWs, the 2003 IBC International Educator of the Year Award, the 2003 IEEE CPMT Outstanding Young Engineer Award for his work on 3-D multilayer integrated RF modules, the 2002 International Conference on Microwave and Millimeter-Wave Technology Best Paper Award (Beijing, China) for his work on compact/SOP-integrated RF components for low-cost high-performance wireless front-ends, the 2002 Georgia Institute of Technology Electrical and Computer Engineering Outstanding Junior Faculty Award, the 2001 ACES Conference Best Paper Award, the 2000 NSF CAREER Award for his work on the development of multiresolution time-domain (MRTD) technique that allows for the system-level simulation of RF integrated modules, and the 1997 Best Paper Award of the International Hybrid Microelectronics and Packaging Society for the development of design rules for low-crosstalk finite-ground embedded transmission lines. He was the recipient/corecipient of the 2007 IEEE AP-S Symposium Best Student Paper Award, the 2007 IEEE IMS Third Best Student Paper Award, the 2007 ISAP 2007 Second Best Poster Presentation Award, the 2006 IEEE MTT-S Outstanding Young Engineer Award, and the 2006 Asia-Pacific Microwave Conference Award.